

Study of a Four-Bed Pressure Swing Adsorption for Oxygen Separation from Air

Moghadazadeh Zahra, Towfighi Jafar, and Mofarahi Masoud

Abstract—This article is presented an experimental and modeling study of a four-bed pressure swing adsorption process using zeolite 13X to provide oxygen-enriched air. The binary mixture N_2/O_2 (79/21 vol %) was used as a feed stream. The effects of purge/feed ratio (P/F), adsorption pressure, cyclic time and product flow rate on product purity and recovery under nonisothermal condition were studied. The adsorption dynamics of process were determined using a mathematical model incorporated mass and energy balances. A Matlab code using finite difference method was developed to solve the set of coupled differential-algebraic equations, and the simulation results are agreed well with experimental results.

Keywords—Pressure swing adsorption (PSA), Oxygen, Zeolite 13X.

I. INTRODUCTION

PRESSURE swing adsorption is one of the most important processes in separation and purification. Purified oxygen is necessary for some application such as medical application, wastewater treatment, chemical processing, etc [1]. Because of this demand, many different processes have expanded to separate oxygen from air, like cryogenic distillation of liquefied air and adsorption processes [2]. Adsorption processes for this subject seems to be the best alternative, because of the maturity of technology, the available adsorbents, and low cost energy (but highly efficient) gas separation system [3]. Therefore, over the last two decades, there has been widespread development of PSA systems. The zeolites A and X are the most important component as an adsorbent in O₂-PSA process [4]. The first and simplest PSA process cycle was suggested by Skarstrom in 1958 [5]. The Skarstrom cycle was included two beds with four steps, pressurization, adsorption, blow down and purge. In 1964, PSA technology was for the first time used to separate oxygen from air [6].

Up to now, many processes with different adsorbents and operational condition were studied for this application. Farooq et al,(1989) used zeolite 5A to separate oxygen from air in a PSA unit performing the Skarstrom cycle. In 1990 Kenny and Liow used 5A zeolite for oxygen separation from air and

studied the effect of pressurization rate, product flow rate and particle size on product purity [7]. Recently, Mendes et al,(2000) focused on the influence on the product purity and recovery of the pressure rising rate during the blow down step and production pressure in O₂-PSA with zeolite 5A [8]. In 2003, a vacuum pressure swing adsorption (VPSA) unit for the production of high-purity oxygen from air, using a new adsorbent, namely AgLiLsx, was described in a patent by Air products and chemicals, Inc[1]. In the latest study for oxygen separation, Mendes et al,(2007) studied about using a silver exchanged zeolite[1].

In the present study a four-bed PSA process using a commercial 13X zeolite is evaluated by experiments and theoretical model. In this process the steps of feed pressurization, production, blowdown, purge, and pressure equalization are included in a cycle. The PSA performances under the same feed rate, adsorption pressure and cycle time were compared by variation of the purge flow and production rate. The adsorption dynamics at each step and the experimental PSA results were predicted by the mathematical model incorporated mass and energy balances.

II. EXPERIMENTAL

The zeolite 13X was obtained from Zheo. Chem. Co. in the form of bead. Adsorbents were activated overnight at 300°C before being used in measurements. The layout of the pilot system is shown in Fig. 1. It contains four columns. The length of each column is 1 meter and its ID is 3 cm. This setup is equipped with an automatic control system for controlling the time of each cycle, for monitoring and recording the flow rate, pressure and column temperature. This system is applicable for a wide range of pressure and adsorbents. The maximum flow rate is 80 lit/min. Changes of pressure in all beds and also in feed and product lines are both monitored and recorded during operation. A Varian Chrompack type GC is used for analyzing feed and product streams. Monitoring and recording the changes of temperature in 3 points of one column and sampling the gas stream inside the columns makes it possible to study the operational conditions of beds carefully. An On/Off control board and a control software designed specifically for this process are used for controlling the process dynamics.

Moghadazadeh Zahra and Towfighi Jafar are with Chemical Engineering Department, Tarbiat Modares University, P.O.Box:14115.143, Tehran, Iran.

Mofarahi Masoud is with Chemical Engineering Department, Persian Gulf University, Bushehr Iran (to whom correspondence should be addressed: Fax:+98 771 4540376 mofarahi@pgu.ac.ir,mofarahi@yahoo.com).

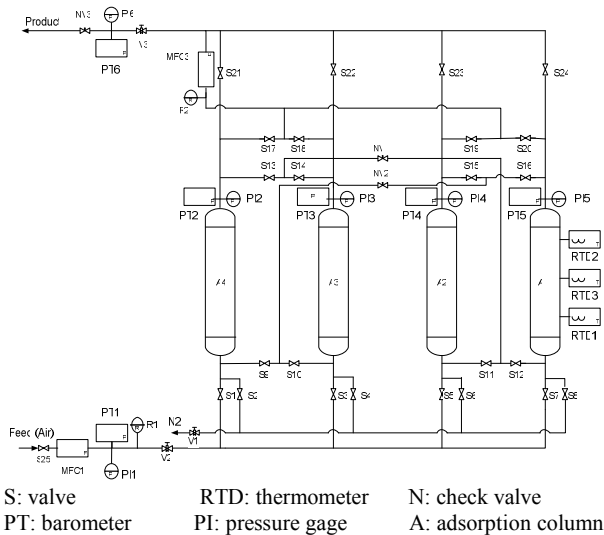


Fig. 1 Schematic diagram of pilot plant

The PSA cycle is consist of 7 steps. These Steps are as follows:

- 1- Pressurization with feed (RF)
- 2- Adsorption (AD)
- 3- Depressurization equalization (ED)
- 4- Blow down (BD)
- 5- Purge (PG)
- 6- Pressurization equalization (EP)
- 7- Idle step (ID)

Idle step is just for adjust the cycle time and no action is occur in this step. Setup sequences of each cycle time for each bed are shown in Table I.

TABLE I
SETUP SEQUENCE

| | | | | | | | | | |
|----|----|----|----|----|----|----|----|----|----|
| A1 | BD | PG | | EP | ID | RF | FD | | ED |
| A2 | FD | ED | BD | PG | | EP | ID | RF | FD |
| A3 | ID | RF | FD | | ED | BD | PG | | EP |
| A4 | PG | EP | ID | RF | FD | | ED | BD | PG |

Characteristics of the adsorption bed and adsorbent are presented in Table II.

Operational condition of PSA process is presented in table III. As it is seen, in 4 different pressures, 3 different cycle time, 4 different P/F ratios and 3 different product rates the tests are taken and the results are available.

III. MATHEMATICAL MODEL

To understand the dynamic behavior of PSA process, the mathematical model by the following assumption were developed.

- 1- The gas phase behaves as an ideal gas.
- 2- The radial concentration gradient is negligible
- 3- The flow pattern is described by the axially dispersed

TABLE II
CHARACTERISTIC OF ADSORPTION BED AND ADSORBENT

| Adsorbent | zeolite 13X |
|---|-------------|
| Adsorbent shape | sphere |
| Adsorbent diameter(mm) | 2-3 |
| Pellet density (gr/cm ³) | 0.93 |
| Heat capacity(KJ/Kg.K) | 1.33 |
| Adsorption Bed | |
| Bed length(m) | 1 |
| Bed internal radius (cm) | 1.5 |
| Bed external radius (cm) | 1.75 |
| Internal heat transfer coefficient(J/m ² .K.s) | 38.45 |
| External heat transfer coefficient(J/m ² .K.s) | 14.212 |

plug-flow model.

4- The mass transfer rate is represented by the LDF model.

5- The pressure drop is negligible.

The component mass balance is described by

$$-D_L \frac{\partial^2 c_i}{\partial z^2} + \frac{\partial(u c_i)}{\partial z} + \frac{\partial c_i}{\partial t} + \rho_p \left(\frac{1-\varepsilon}{\varepsilon} \right) \frac{\partial \bar{q}_i}{\partial t} = 0 \quad (1)$$

And the overall mass balance represents by

$$\frac{\partial(u C)}{\partial z} + \frac{\partial C}{\partial t} + \rho_p \left(\frac{1-\varepsilon}{\varepsilon} \right) \sum_{i=1}^n \frac{\partial \bar{q}_i}{\partial t} = 0 \quad (2)$$

The energy balance can be represented as follows

$$-K_L \frac{\partial^2 T}{\partial z^2} + \varepsilon \rho_g C_{Pg} \frac{\partial(u T)}{\partial z} + (\varepsilon_i \rho_g C_{Pg} + \rho_B C_{Ps}) \frac{\partial T}{\partial t} - \rho_B \sum_{i=1}^n (-\Delta H_i) \frac{\partial \bar{q}_i}{\partial t} + \frac{2h_i}{R_{Bi}} (T - T_w) = 0 \quad (3)$$

And the energy balance for considering the heat loss through the bed wall is described by

$$\rho_w C_{Pw} A_w \frac{\partial T_w}{\partial t} = 2\pi R_{Bi} h_i (T - T_w) - 2\pi R_{Bo} h_o (T_w - T_{atm}) \quad (4)$$

Where $A_w = \pi (R_{Bo}^2 - R_{Bi}^2)$

The initial and boundary conditions are presented below.

Feed pressurization and adsorption steps

$$-D_L \frac{\partial C_i}{\partial z} \Big|_{z=0} = u (c_i|_{z=0^-} - c_i|_{z=0^+}) \quad (5)$$

$$\frac{\partial c_i}{\partial z} \Big|_{z=L} = 0$$

TABLE III
OPERATION CONDITION OF PSA PROCESS

| Pressure(bar) | Cycle time(S) | P/F ratio | product(lit/min) |
|---------------|---------------|-----------|------------------|
| 3.5 | 180 | 0.1 | 0.5 |
| | | 0.16 | 0.75 |
| | | 0.2 | 1 |
| | | 0.24 | |
| | 160 | 0.1 | 0.5 |
| | | 0.16 | 0.75 |
| | | 0.2 | 1 |
| | | 0.24 | |
| | 140 | 0.1 | 0.5 |
| | | 0.16 | 0.75 |
| | | 0.2 | 1 |
| | | 0.24 | |
| 4 | 180 | 0.1 | 0.5 |
| | | 0.16 | 0.75 |
| | | 0.2 | 1 |
| | | 0.24 | |
| | 160 | 0.1 | 0.5 |
| | | 0.16 | 0.75 |
| | | 0.2 | 1 |
| | | 0.24 | |
| | 140 | 0.1 | 0.5 |
| | | 0.16 | 0.75 |
| | | 0.2 | 1 |
| | | 0.24 | |
| 4.5 | 180 | 0.1 | 0.5 |
| | | 0.16 | 0.75 |
| | | 0.2 | 1 |
| | | 0.24 | |
| | 160 | 0.1 | 0.5 |
| | | 0.16 | 0.75 |
| | | 0.2 | 1 |
| | | 0.24 | |
| | 140 | 0.1 | 0.5 |
| | | 0.16 | 0.75 |
| | | 0.2 | 1 |
| | | 0.24 | |
| 5 | 180 | 0.1 | 0.5 |
| | | 0.16 | 0.75 |
| | | 0.2 | 1 |
| | | 0.24 | |
| | 160 | 0.1 | 0.5 |
| | | 0.16 | 0.75 |
| | | 0.2 | 1 |
| | | 0.24 | |
| | 140 | 0.1 | 0.5 |
| | | 0.16 | 0.75 |
| | | 0.2 | 1 |
| | | 0.24 | |
| 6.5 | 180 | 0.6 | 0.5 |
| | | 0.13 | 0.75 |
| | | 0.20 | 1.25 |
| | | | |
| | 140 | 0.6 | 0.5 |
| | | 0.13 | 0.75 |
| | | 0.20 | 1.25 |
| | | | |

$$-K_L \frac{\partial T}{\partial z} \Big|_{z=0} = uc_{pg} \rho_g (T|_{z=0^-} - T|_{z=0^+})$$

(6)

$$\frac{\partial T}{\partial z} \Big|_{z=L} = 0$$

Where $c_i|_{z=0^-}$ is the feed composition for component i.

Purge and pressurizing pressure equalization steps

$$-D_L \frac{\partial C_i}{\partial z} \Big|_{z=L} = u(c_i|_{z=L^+} - c_i|_{z=L^-})$$

(7)

$$\frac{\partial c_i}{\partial z} \Big|_{z=0} = 0$$

$$-K_L \frac{\partial T}{\partial z} \Big|_{z=L} = uc_{pg} \rho_g (T|_{z=L^+} - T|_{z=L^-})$$

(8)

$$\frac{\partial T}{\partial z} \Big|_{z=0} = 0$$

Where $c_i|_{z=L^+}$ is the volume average of effluent stream during adsorption step.

Depressurizing pressure equalization and countercurrent depressurization steps

$$\frac{\partial c_i}{\partial z} \Big|_{z=0} = \frac{\partial c_i}{\partial z} \Big|_{z=L} = 0$$

(9)

$$\frac{\partial T}{\partial z} \Big|_{z=0} = \frac{\partial T}{\partial z} \Big|_{z=L} = 0$$

(10)

The initial condition is represented by

$$c_i(z,0) = 0$$

(11)

$$q_i(z,0) = 0$$

(12)

The sorption rate is described by LDF model with the single lumped mass transfer parameter

$$\frac{\partial \bar{q}_i}{\partial t} = k(q_i^* - \bar{q}_i)$$

(13)

The extended Langmuir-Freundlich isotherm is used to predict the multi component adsorption equilibrium

$$q_i = \frac{q_{mi} B_i P_i^{n_i}}{1 + \sum_{j=1}^n B_j P_j^{n_j}}$$

(14)

Where $q_m = k_1 + k_2 T$, $B = k_3 \exp(k_4/T)$, and $n_i = k_5 + k_6/T$.

The isotherm parameters are listed in Table IV.

TABLE IV
ISOTHERM PARAMETERS

| | N | O |
|-------|-----------|-----------|
| | 2 | 2 |
| k_1 | 12.52 | 6.705 |
| k_2 | -0.01785 | -0.01435 |
| k_3 | 0.0002154 | 0.0003253 |
| k_4 | 2333 | 1428 |
| k_5 | 1.666 | -0.3169 |
| k_6 | -245.2 | 387.8 |

A finite difference method (FDM) was used to solve a mathematical model that considered of coupled partial differential equations. The spatial dimension was discretized by using a second order central difference and a second order

backward difference for the second order and the first order space derivatives. Solving of algebraic equations were done by Matlab software.

IV. RESULT AND DISCUSSION

All Figs. for the final node in adsorption bed have presented as below. In Fig. 2 the temperature variations in one cycle and different steps of a cycle time is shown.

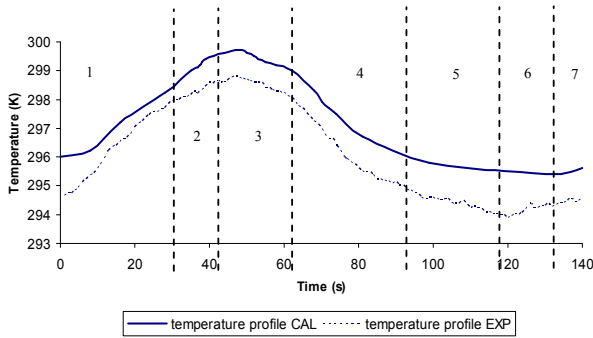


Fig. 2 Temperature profile in cycle time of 140 s

The first step is adsorption and other steps are coming respectively. As we can see, the changes are very negligible and the isothermal assumption could be a good assumption for these processes.

Purity variation versus purge is presented in Fig. 3.

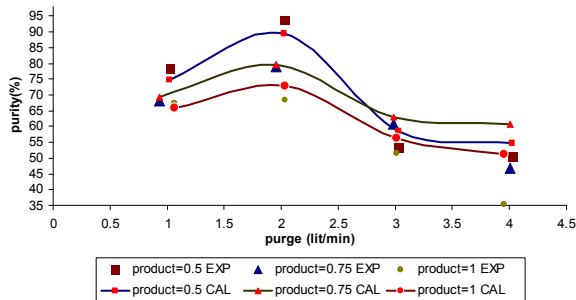


Fig. 3 Purity variations versus purge in a cycle time of 180 s and the pressure of 4 bars

Purity is increased with increasing of purge and after reaching to a peak, decreasing. As we know, purging the adsorption bed, help the adsorbent regeneration and increase its capability, but increasing the amount of this stream more than its sufficiency causes the adsorption of oxygen on the adsorbent because of its high vapor pressure in the column and the efficiency of adsorbent will be decreased.

With increase in the product amount, the peak of purity is coming down. Large amount of product stream is because of large amount of feed stream. The large amount of feed stream, the low efficiency separating of feed stream, because of large volume of gas in the adsorption bed at the same time.

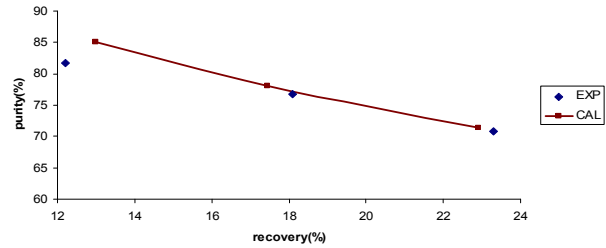


Fig. 4 Purity versus recovery for cycle time of 140 s and purge of 1 lit/min and pressure of 4 bars

Purity versus recovery is a descent function. The higher the purity has the lower the recovery. For increasing the purity, decreasing the amount of feed stream can be helpful, because lower amount can be separated well in neighborhood of adsorbent but recovery will be decreased because of low amount of entrance feed stream and visa versa.

The same results were seen for other cycle times.

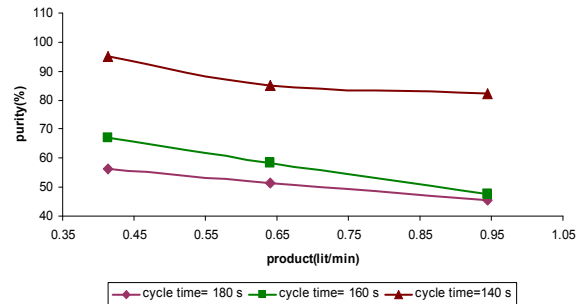


Fig. 5 Purity versus product in different cycle times and P/F = 0.2

As we can see in Fig. 5, in short cycle time, higher purity will be achieved. Because there is not enough time for oxygen adsorption instead of nitrogen. On the other hand, profiles for long cycle times with increasing the product, decreases more quietly, since the long adsorption time supplies enough time for separating the high amount of feed stream.

As a result we can say, with increasing the product flow rate, the purity will decrease and it's because of higher feed flow rate.

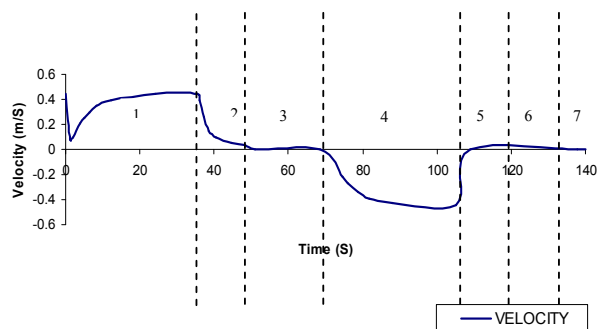


Fig. 6 Velocity profile in one cycle of cycle time of 140 s and the initial value of 0.448 m/s

Velocity profile in one cycle of cycle time of 140 s is shown in Fig. 6. As mentioned above, velocity values at the end of the adsorption bed is drawn. The first step is adsorption step and other steps are come respectively.

In the fourth step, purge, the negative velocity is because of converse direction of entrance stream.

In steps 3 and 5 to 7, the velocity will be zero. Because of the closed terminal valve of the adsorption bed.

Entrance velocity at purge step is the exit point velocity of the adsorption step but in the converse direction.

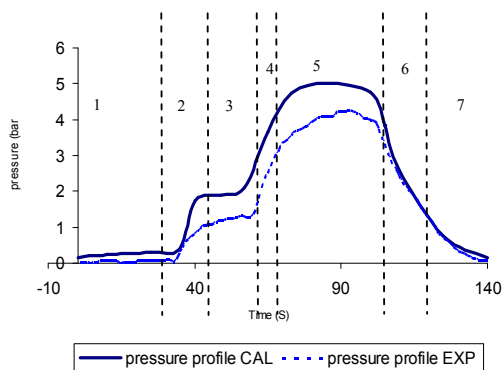


Fig. 7 Pressure profile in one cycle of cycle time of 140 s

As we can see in Fig. 7, the experimental results are agreed well with the calculating results.

Total concentration profile behaves like pressure profile, since we assumed gas phase behaves as an ideal gas.

The first step in this figure is purge step and others come respectively. In purge and adsorption step, total pressure or total concentration is constant and in other steps is variable.

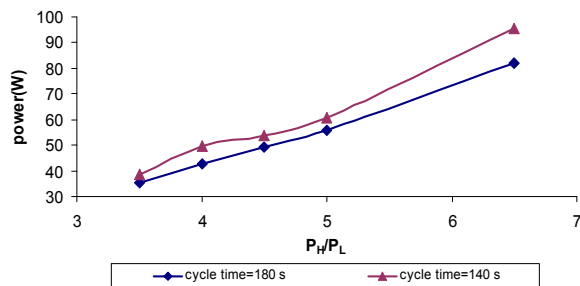


Fig. 8 Power versus pressure ratio in 2 cycle times of 180 s and 140 s

The using equation for power calculation is presented below.

$$\dot{W} = \frac{\gamma}{\gamma - 1} \frac{\dot{m} RT}{\eta} \left(\left(\frac{P_H}{P_L} \right)^{\frac{\gamma-1}{\gamma}} - 1 \right) \quad (15)$$

In Fig. 8 comparison of power for two different cycle times is presented. As it shows, the consuming power for short cycle time is more than long cycle time.

Because of the short duration step times in short cycle time,

compressor should be compressed the entrance feed in several times, more than long cycle time and the required energy will be increased.

In addition, with increasing the pressure ratio, the required power increases. As we know, good performance of adsorption processes depends on pressure. Because of this fact, we try to increase the pressure. On the other hand, increasing the pressure causes enlargement in cost. Then an optimum situation is needed for commercial processes.

REFERENCES

- [1] Santos J.C., Cruz P, Regala T., Magalhaes F.D., and Mendes A., "High-Purity Oxygen Production by Pressure Swing Adsorption", *Ind Eng chem* 46, 2007, pp 591-599.
- [2] Salil U. Rege, Ralph T. Yang, Kangyi Qian, Mark A. Buzanowski, "Air-Purification by Pressure Swing Adsorption Using Single/Layered Beds", *chemical engineering science* 56, 2001, pp 2745-2759.
- [3] Mofarah Masoud, Sadrameli Mojtaba, Towfighi Jafar, "Four-bed Vacuum Pressure Swing Adsorption Process for Propylene/Propane Separation", *Ind Eng chem.* 44, 2005, pp1557-1564.
- [4] Yoshida S., Ogawa N., Kamioka K., Hirano S, and Mori, T. "Study of Zeolite Molecular Sieves for Production of Oxygen by Using Pressure Swing Adsorption", Kluwer Academic Publisher, 5, 1999, pp 57-61.
- [5] Subramanian Dharmashankar, Ritter, James, Yujun Liu A., "Equilibrium Theory for Solvent Vapor Recovery by Pressure Swing Adsorption: Analytic Solution with Velocity Variation and Gas-phase Capacity", *chemical engineering science*, 54, 1999, pp 475-481.
- [6] Adelio M. M Mendes, Carlos A.V. Costa, Alirio E. Rodrigues, "Oxygen Separation from Air by PSA: Modeling and Experimental Results Part I: Isothermal Operation", *separation and purification technology*, 24, 2001, pp173-188.
- [7] Liow J., Kenny C.N, "The Backfill Cycle of the Pressure Swing Adsorption Process", *AIChE J.*36, 1990, 53.
- [8] Jee Jeong-Geun, Lee Jong-Seok, and Lee Chang-Ha, "Air Separation by a Small-Scale Two-Bed Medical O2 Pressure Swing Adsorption", *Ind .En Chem.Res.*40, 2001, 3647-3658.